Caliphate Journal of Science & Technology (CaJoST)

ISSN: 2705-313X (**PRINT**); 2705-3121 (**ONLINE**) **Research Article**

Article Info

Received: 9th January 2019

Revised: 15th February 2019

Accepted: 18th February 2019

[1]Department of Mathematical Science, Federal University Gusau, zamfara State, Nigeria. P.M.B.
[2,3]Department of Mathematics, Federal University Birnin Kebbi, Kebbi State, Nigeria. P.M.B. 1157

***Corresponding author's email:** emmanuelomokhuale@yahoo.com

Cite this: *CaJoST,* 2019, 1, 61-70

Unsteady Heat and Mass Transfer Magnetohydrodynamic (MHD) Convective Couette Flow with Thermal Radiation using Finite Element Method (FEM)

Emmanuel Omokhuale[1]*, Muhammad M. Altine[2], and Anas Yusuf[3]

An analysis of unsteady hydromagnetic convective Couette flow of a viscous, electrically conducting and incompressible fluid taking into cognizance thermal radiation, diffusion and diffusion thermo effects is conducted numerically using Finite Element Method (FEM). Computations were done for a wide range of parameters of engineering interest embedded in the flow problem. The effects of these flow parameters on the velocity, temperature and concentration are presented graphically while that of the skin-friction, the obtained results are benchmarked with previously published works and was seen to be in good agreement.

Keywords: Magnetohydrodynamics; Free convection; Finite Element Method; Heat and mass transfer

1. Introduction

Many physical situations find the existence of Convection flow such as in the study of environmental heat transfer processes and in the cooling of nuclear reactors etc. There are three (3) forms namely: free, mixed and forced. Free convection is most significant owing to its usefulness in numerous engineering applications. For example, in an automatic control system that comprise of electrical and electronic components that is constantly subjected to periodic heating and cooled by free convection process. [1] reported natural convection Couette flow of a reactive viscous fluid in a vertical channel. [2] examined combined effects of magnetic field and chemical reaction on unsteady natural convective flow in a vertical in a vertical channel.

MHD free convective Couette flow has been studied with focus to its significance in several industrial problems. For example, in the power industry, among the methods of generating electric power is one in which electrical energy is extracted directly from a moving conducting fluid. [3] examined free convection effects on steady MHD flow past a vertical porous plate. Hossain *et al.* (1998) investigated the effect of radiation on free convection from a porous vertical plate. Some recent studies containing the free convection phenomenon can be seen in [4], [5], [6], [7]. [8] studied MHD free convection flow of a non-Newtonian fluid past an infinitely started vertical plate numerically. In particular, free convection flows in porous medium has attracted great attention in recent years due to their relevance in the field of science and engineering such as geothermal systems, thermal insulations, solid matrix exchangers, oil extraction and to store waste materials. [9]) and [10] and many other authors have contributed in this field. Convective heat transfer plays an important role in processing of non-Newtonian fluid flows. Mechanics of non-Newtonian fluid flows present a special challenge to engineers, physicists and mathematicians.

The heat transfer affected because of concentration difference is referred to as Diffusion-thermo effect. On the other hand, mass transfer affected because of temperature gradient is known as Thermal-diffusion effect. [11] studied unsteady hydromagnetic natural convection Couette flow of a viscous, incompressible and electrically conducting fluid between two vertical plates in the presence of thermal radiation using finite element method. [12] examined steady state MHD Couette flow of a viscous, incompressible and electrically conducting fluid flow between two infinite parallel plates in the presence of an inclined magnetic field. [13] analyzed flow formation in Couette motion in magnetohydrodynamics with time varying suction and taking into consideration the effects of heat and mass transfer. [14] analyzed MHD Couette

motion of an electrically conducting, viscous incompressible fluid through saturated porous medium bounded by two insulated vertical porous plate. [15] presented unsteady MHD free convective Couette flow between two infinite vertical porous plate in the presence of transverse magnetic field and thermal radiation numerically using finite difference method. [16] studied heat and mass transfer of a viscoelastic fluid in a fixed plane. [17] analyzed heat and mass transfer with periodic suction and heat sink. [18] discussed variable thermal conductivity effect with Jeffery fluid using finite difference method.

Finite Element Method (FEM) is a numerical technique used to obtain an approximate solution to boundary value problems as they consist of elliptic partial differential equations and the boundary conditions. It has been applied to many physical problems. The method basically consists of assuming the piecewise continuous function for the solution and obtaining the parameters of the functions in a manner that reduces the error of the solution. [19] found out effect of Jeffery on heat and mass transfer with Soret and variable thermal conductivity. [20] presented effects of Dufour and heat source on free convection flow.

Using FEM, [21] examined heat and mass transfer in MHD flow of a viscous fluid past a vertical plate under oscillatory suction velocity. [22] investigated unsteady MHD heat transfer in Couette flow of water at 4^{O}C in a rotating system with ramped temperature. [23] studied unsteady radiative MHD natural convection Couette flow between permeable plates. Recently, [24] analyzed a Couette flow of conducting fluid.

Motivated by the above studies and applications, a novel investigation has been conducted to study unsteady free convective MHD Couette flow with heat and mass transfer in the presence of thermal radiation. The flow is governed by a modeled coupled nonlinear system of partial differential equations (PDEs) in dimensional form which are transformed into non-dimensional form using some suitable non-dimensional variables. The resulting ordinary differential equations (ODEs) in non-dimensional form were solved numerically by FEM to obtain approximate solutions for the velocity, temperature and concentration. Furthermore, the effects of physical parameters embedded in the problem were examined with the help of graphs.

2. Mathematical Formulation

Two dimensional unsteady convective Couette flow of a viscous, electrically conducting fluid past a porous plate under the influence of a uniform magnetic field, heat and mass transfer with thermal radiation. The assumptions stated below are considered: (i) The x^*-axis and y^*- axis are taken along the plate in the vertical upward and normal direction to the plate respectively. (ii) The transverse magnetic field of uniform strength B_o is to be applied normal to the plate. (iii) The fluid has constant thermal conductivity and kinematic viscosity, the Boussinesq approximation has been taken for the flow.

From the above assumptions, the unsteady flow is governed by the following partial differential equations.

Momentum equation:

$$\frac{\partial u^*}{\partial t^*} = \nu \frac{\partial^2 u^*}{\partial y^{*2}} + g\beta_T \left(T^* - T_H^*\right) + g\beta_m \left(T^* - T_H^*\right) - \frac{\sigma \mu_e^2 B_0^2}{\rho}\left(u^* - U_0 t^{*n}\right) \quad (1)$$

Energy equation:

$$\frac{\partial T^*}{\partial t^*} = \frac{k_0}{\rho Cp}\frac{\partial^2 T^*}{\partial y^{*2}} + \frac{D_m k_T}{c_s c_p}\frac{\partial^2 C^*}{\partial y^{*2}} - \frac{1}{\rho Cp}\frac{\partial q_r}{\partial y'} - Q_0\left(T^* - T_H^*\right) \quad (2)$$

Species diffusion equation:

$$\frac{\partial C^*}{\partial t^*} = Dc\frac{\partial^2 C^*}{\partial y^{*2}} - \frac{D_m k_T}{T_m}\frac{\partial^2 T^*}{\partial y^{*2}} - Rc\left(C^* - C_H^*\right) \quad (3)$$

The corresponding initial and boundary conditions are:

$$\left.\begin{array}{l} t^* \le 0 : u^* = 0, T^* = T_H^*, C^* = C_H^* \quad for \;\; 0 \le y^* \le H \\ t^* > 0 : \begin{cases} u^* = U_0 t^{*n}, T^* = T_w^*, C^* = C_w^* \quad at \; y^* = 0 \\ u^* = 0, T^* = T_H^*, C^* = C_H^* \quad at \;\; y^* = H \end{cases} \end{array}\right\} \quad (4)$$

The radiative heat flux is reduced by employing the Rosseland approximation given as

$$q_r = -\frac{4\sigma^*}{3k^*}\frac{\partial T^{*4}}{\partial y^*} \quad (5)$$

we assume that the difference in temperature within the flow are sufficiently small such that q_r may be presented as a linear function of T^*.

Therefore, on expanding T^{*4} in Taylor series about T_H^* up to first order approximation, gives

$$T^{*4} = T_H^* + 4\left(T^* - T_H^*\right)T_H^{*3} = 4T^*T_H^{*3} - 3T_H^{*4} \quad (6)$$

Using Equations (5) and (6) in the last term of Eq. (2), we get:

$$\frac{\partial q_r}{\partial y^*} = -\frac{16\sigma T_H^{*3}}{3k^*}\frac{\partial^2 T^*}{\partial y^{*2}} \quad (7)$$

Introducing (7) into Eq. (2), the energy equation becomes:

$$\frac{\partial T^*}{\partial t^*} = \frac{k_0}{\rho Cp}\frac{\partial^2 T^*}{\partial y^{*2}} + \frac{D_m k_T}{c_s c_p}\frac{\partial^2 C^*}{\partial y^{*2}} + \frac{16\sigma T_H^{*3}}{3k^*\rho Cp}\frac{\partial^2 T^*}{\partial y^{*2}} + Q_0\left(T^* - T_H^*\right) \quad (8)$$

Introducing the following dimensionless quantities in Equations (1), (3) and (8) we have

$$\left.\begin{array}{l} U = \frac{u^*}{H}, Y = \frac{y^*}{H}, t = \frac{t^*\nu}{H^2}, T = \frac{T^* - T_H^*}{T_w^* - T_H^*}, C = \frac{C^* - C_H^*}{C_w^* - C_H^*}, \\ Gr = \frac{g\beta_T\left(T_w^* - T_H^*\right)}{\nu}, Gc = \frac{g\beta_m\left(C_w^* - C_H^*\right)}{\nu}, F = \frac{U_0 H^{2n-1}}{\nu^n} \\ M^2 = \frac{\sigma\mu_e^2 B_0^2 H^2}{\rho\nu}, R = \frac{3k_0 k^*}{4\sigma T_H^{*3}}, \Pr = \frac{\rho\nu Cp}{k_0}, Sc = \frac{\nu}{D}, \\ Dr = \frac{D_m k_T H^2\left(C_w^* - C_H^*\right)}{\nu c_s c_p\left(T_w^* - T_H^*\right)}, Sr = \frac{D_m k_T\left(T_w^* - T_H^*\right)}{\nu T_m\left(C_w^* - C_H^*\right)}, \mathrm{Re}_x^{-1} = \frac{U_0 x^*}{\nu} \end{array}\right\} \quad (9)$$

Substituting equation in to (1), (3) and (8), the equations reduces to the following dimensionless form of equations

$$\frac{\partial U}{\partial t} = \frac{\partial^2 U}{\partial Y^2} + GrT + GcC - M^2\left(U - Ft^n\right) \quad (10)$$

$$\frac{\partial T}{\partial t} = \frac{1}{\Pr}\left(\frac{3R+4}{3R}\right)\frac{\partial^2 T}{\partial Y^2} + Dr\frac{\partial^2 C}{\partial Y^2} + ST \quad (11)$$

$$\frac{\partial C}{\partial t} = \frac{1}{Sc}\frac{\partial^2 C}{\partial Y^2} + Sr\frac{\partial^2 T}{\partial Y^2} - RcC \quad (12)$$

Using equation (9), the initial and boundary conditions (4) reduce to

$$\left.\begin{array}{l} t \le 0 : U = 0, T = 0, C = 0 \quad for \quad 0 \le Y \le H \\ t > 0 : \begin{cases} U = Ft^n, T = 1, C = 1 & at\, Y = 0 \\ U = 0, T = 0, C = 0 & at\ Y = H \end{cases} \end{array}\right\} \quad (13)$$

Two cases are studied, to find the solutions of equations (10), (11) and (12) subject to the initial and boundary conditions (13):

1. Impulsive movement of the plate at $Y = 0$ (i.e, $n = 0$) and
2. Uniform accelerated movement of the plate at $Y = 0$ (i.e, $n = 1$).

Case (1): Impulsive movement of the plate at $Y = 0$:

Taking $n = 0$ in equation (10), then the equation can be expressed as

$$\frac{\partial U}{\partial t} = \frac{\partial^2 U}{\partial Y^2} + GrT + GcC - M^2\left(U - F\right) \quad (14)$$

and the corresponding boundary conditions (13) reduce to

$$\left.\begin{array}{l} t \le 0 : U = 0, T = 0, C = 0 \quad for \quad 0 \le Y \le H \\ t > 0 : \begin{cases} U = F, T = 1, C = 1 & at\, Y = 0 \\ U = 0, T = 0, C = 0 & at\ Y = H \end{cases} \end{array}\right\} \quad (15)$$

Case (2): Uniform accelerated movement of the plate at $Y = 0$.

Taking $n = 1$ in equation (10), then it can be written as

$$\frac{\partial U}{\partial Y} = \frac{\partial^2 U}{\partial Y^2} + GrT + GcC - M^2\left(U - Ft\right) \quad (16)$$

and the initial and boundary conditions (13) reduce to

$$\left.\begin{array}{l} t \le 0 : U = 0, T = 0, C = 0 \quad for \quad 0 \le Y \le H \\ t > 0 : \begin{cases} U = Ft, T = 1, C = 1 & at\, Y = 0 \\ U = 0, T = 0, C = 0 & at\ Y = H \end{cases} \end{array}\right\} \quad (17)$$

For practical engineering applications and the design of chemical engineering systems, quantities of interest viz. Skin-friction, Nusselt and Sherwood numbers which are necessary to compute. The skin-friction or the shear tress at the moving plate of the channel in dimensionless form is given by

$$\tau = -\left(\frac{\tau_w^*}{\rho u_0 \nu}\right)_{y^*=0} = -\left(\frac{\partial U}{\partial Y}\right)_{y^*=0} \quad (18)$$

The rate of heat transfer at the moving hot plate of the channel in dimensionless form is illustrated by

$$Nu_0 = -x^* \frac{\left(\frac{\partial T^*}{\partial Y^*}\right)_{y^*=0}}{T_w^* - T_H^*} \Rightarrow Nu_0 \,\mathrm{Re}_x^{-1} = -\left(\frac{\partial T}{\partial Y}\right)_{Y=0} \quad (19)$$

Also, the rate of heat transfer on the stationary plate is given by

$$Nu_1 = -x^* \frac{\left(\frac{\partial T^*}{\partial Y^*}\right)_{y^*=H}}{T_w^* - T_H^*} \Rightarrow Nu_1 \,\mathrm{Re}_x^{-1} = -\left(\frac{\partial T}{\partial Y}\right)_{Y=1} \quad (20)$$

The Sherwood number at the moving plate of the channel in dimensionless form is given by

$$Sh = -x^* \frac{\left(\frac{\partial C^*}{\partial Y^*}\right)_{y^*=0}}{C_w^* - C_H^*} \Rightarrow Sh\,\mathrm{Re}_x^{-1} = -\left(\frac{\partial C}{\partial Y}\right)_{Y=0} \quad (21)$$

where Re_x is the Reynold's number. The mathematical modelling of the problem is now done. So, Eqs. (11), (12), (14) and (16) presents a coupled system of linear PDEs and these are to be solved with initial and boundary conditions (15) and (17). Therefore, finding the exact solutions are complicated, whenever it is possible. Thus, these equations are solved numerically by finite element method.

3. Method of Solution by Finite Element Method

3.1 Numerical solutions by Finite Element Method

The Finite Element Method (FEM) is an efficient numerical and computational method to solving a variety of engineering and real-world problems. So many developers, researchers and users have recognized this method as one of the most powerful numerical analysis tools useful to analyze complex engineering problems. The simplicity, flexibility, computability and accuracy of the method make it significant in modelling and design process. This is because of the discretization of domain of the problem is done employing highly flexible elements or uniform or non-uniform patches that can be easily shown as complex shapes. The method vitally comprises the piecewise continuous functions in a systematic way that reduces the error in the solution.

The steps involved in the finite element analysis as follows:

Step 1: Discretization of the domain
Step 2: Generation of the element equations
Step 3: Assembling of the element equations
Step 4: Imposition of the boundary conditions
Step 5: Solution of assembled equations

3.2 Variational Formulation

The Variational formulation associated with Eqs. (10) – (12) over a typical two-noded linear element $\left(Y_e, Y_{e+1}\right)$ is given by

$$\int_{Y_e}^{Y_{e+1}} z_1 \left[\left(\frac{\partial U}{\partial t}\right) - \left(\frac{\partial^2 U}{\partial y^2}\right) - Gr(T) - Gc(C) + M^2\left(U - Ft^n\right)\right] dy = 0 \quad (22)$$

$$\int_{Y_e}^{Y_{e+1}} z_2 \left[\left(\frac{\partial T}{\partial t}\right) - \frac{1}{\mathrm{Pr}}\left(\frac{3R+4}{3R}\right)\left(\frac{\partial^2 T}{\partial y^2}\right) - Dr\left(\frac{\partial^2 C}{\partial y^2}\right) - ST\right] dy = 0 \quad (23)$$

$$\int_{Y_e}^{Y_{e+1}} z_3 \left[\left(\frac{\partial C}{\partial t}\right) - \frac{1}{Sc}\left(\frac{\partial^2 C}{\partial y^2}\right) - Sr\left(\frac{\partial^2 T}{\partial y^2}\right) - RcC\right] dy = 0 \quad (24)$$

where z_1, z_2 and z_3 are arbitrary test functions and may be seen as the variation in U, T and C respectively. When the order of integration was reduced, we got the following system of equations:

$$\int_{Y_e}^{Y_{e+1}} z_1 \left[z_1\left(\frac{\partial U}{\partial t}\right) + \left(\frac{\partial z_1}{\partial y^2}\right)\left(\frac{\partial U}{\partial y}\right) + \left(M^2\right)\left(z_1\right)U - \left(F\right)\left(z_1\right)t^n - \left(Gr\right)\left(z_1\right)T - \left(Gc\right)\left(z_1\right)C\right] dy$$

$$- \left[\left(z_1\right)\left(\frac{\partial u}{\partial y}\right)\right]_{Y_e}^{Y_{e+1}} = 0 \quad (25)$$

$$\int_{Y_e}^{Y_{e+1}} \left[\left(z_2\right)\left(\frac{\partial T}{\partial t}\right) + \frac{1}{\mathrm{Pr}}\left(\frac{3R+4}{3R}\right)\left(\frac{\partial z_2}{\partial y}\right)\left(\frac{\partial T}{\partial y}\right) + Dr\left(\frac{\partial z_2}{\partial y}\right)\left(\frac{\partial C}{\partial y}\right)\right] dy$$

$$- \left[\left(\frac{z_2}{\mathrm{Pr}}\right)\left(\frac{\partial T}{\partial y}\right) + Dr\left(z_2\right)\left(\frac{\partial T}{\partial y}\right)\right]_{Y_e}^{Y_{e+1}} = 0 \quad (26)$$

$$\int_{Y_e}^{Y_{e+1}} \left[\left(z_3\right)\left(\frac{\partial C}{\partial t}\right) + \frac{1}{Sc}\left(\frac{\partial z_3}{\partial y}\right)\left(\frac{\partial C}{\partial y}\right) + Sr\left(\frac{\partial z_3}{\partial y}\right)\left(\frac{\partial T}{\partial y}\right)\right] dy$$

$$- \left[\left(\frac{z_3}{Sc}\right)\left(\frac{\partial C}{\partial y}\right) + Sr\left(z_3\right)\left(\frac{\partial C}{\partial y}\right)\right]_{Y_e}^{Y_{e+1}} = 0 \quad (27)$$

3.3 Finite Element Formulation

The finite element model can be gotten from Eqs. (25) – (27) by substituting the finite element approximations of the form:

$$U=\sum_{k=1}^{2}U_k^e\xi_k^e, T=\sum_{k=1}^{2}T_k^e\xi_k^e \text{ and } \sum_{k=1}^{2}C_k^e\xi_k^e \quad (28)$$

with $z_1=z_2=z_3=\xi_k^e\left(k=1,2\right), U_k^e, T_k^e$ and C_k^e

are the velocity, temperature and concentration respectively at the k^{th} node of typical e^{th} element $\left(Y_e, Y_{e+1}\right)$ and ξ_k^e are the shape functions for this element $\left(Y_e, Y_{e+1}\right)$ and are taken as:

$$\xi_1^e=\frac{Y_{e+1}-Y}{Y_{e+1}-Y_e}$$

and $\xi_2^e=\dfrac{Y-Y_e}{Y_{e+1}-Y_e},\ Y_e\le Y\le Y_{e+1}$ (29)

This finite element model of the equations for

$$\begin{bmatrix}[P^{11}] & [P^{12}] & [P^{13}]\\ [P^{21}] & [P^{22}] & [P^{23}]\\ [P^{31}] & [P^{32}] & [P^{33}]\end{bmatrix}\begin{Bmatrix}\{U^e\}\\ \{T^e\}\\ \{C^e\}\end{Bmatrix}+\begin{bmatrix}[W^{11}] & [W^{12}] & [W^{13}]\\ [W^{21}] & [W^{22}] & [W^{23}]\\ [W^{31}] & [W^{32}] & [W^{33}]\end{bmatrix}\begin{Bmatrix}\{U'^e\}\\ \{T'^e\}\\ \{C'^e\}\end{Bmatrix}=\begin{Bmatrix}\{a^{1e}\}\\ \{a^{2e}\}\\ \{a^{3e}\}\end{Bmatrix} \quad (30)$$

where $\left\{\left\{P^{mn}\right\},\left\{W^{mn}\right\}\right\}$ and

$\left\{\left\{U^e\right\},\left\{T^e\right\},\left\{C^e\right\},\left\{U'^e\right\},\left\{T^e\right\},\left\{C^e\right\},\left\{a^{me}\right\}\right\}\left(m=1,2,3\right)$ are the set of matrices of order 2×2 and 2×1 respectively and $'$ (dash) indicates $\dfrac{d}{dy}$.

These matrices are defined as follows:

$$P_{ik}^{11}=\int_{Y_e}^{Ye+1}\left[\left(\frac{\partial\xi_i^e}{\partial y}\right)\left(\frac{\partial\xi_k^e}{\partial y}\right)\right]dy+\left(M^2\right)\int_{Y_e}^{Ye+1}\left[\left(\xi_i^e\right)\left(\xi_k^e\right)\right]dy-Ft^n\int_{Y_e}^{Ye+1}\left(\xi_i^e\right)dy,$$

$$P_{ik}^{12}=-Gr\int_{Y_e}^{Ye+1}\left[\left(\xi_i^e\right)\left(\xi_k^e\right)\right]dy, P_{ik}^{13}=-Gc\int_{Y_e}^{Ye+1}\left[\left(\xi_i^e\right)\left(\xi_k^e\right)\right]dy, W_{ik}^{11}=\int_{Y_e}^{Ye+1}\left[\left(\xi_i^e\right)\left(\xi_k^e\right)\right]dy, W_{ik}^{12}=W_{ik}^{13}=0,$$

$$W_{ik}^{21}, W_{ik}^{23}=0, W_{ik}^{31}=W_{ik}^{32}=0, P_{ik}^{21}=0, P_{ik}^{31}=0, b_i^{1e}=\left[\left(\xi_i^e\right)\left(\frac{\partial U}{\partial Y}\right)\right]_{Y_e}^{Y_{e+1}}$$

$$P_{ik}^{22}=\frac{1}{\Pr}\left(\frac{3R+4}{3R}\right)\int_{Y_e}^{Ye+1}\left[\left(\frac{\partial\xi_i^e}{\partial Y}\right)\left(\frac{\partial\xi_k^e}{\partial Y}\right)\right]dy, P_{ik}^{23}=Du\int_{Y_e}^{Ye+1}\left[\left(\frac{\partial\xi_i^e}{\partial Y}\right)\left(\frac{\partial\xi_k^e}{\partial Y}\right)\right]dy,$$

$$P_{ik}^{33}=\frac{1}{Sc}\int_{Y_e}^{Ye+1}\left[\left(\frac{\partial\xi_i^e}{\partial Y}\right)\left(\frac{\partial\xi_k^e}{\partial Y}\right)\right]dy, W_{ik}^{22}\int_{Y_e}^{Ye+1}\left[\left(\xi_i^e\right)\left(\xi_k^e\right)\right]dy,$$

$$a_i^{2e}=\left[\left(\frac{\xi_i^e}{\Pr}\right)\left(\frac{3R+4}{3R}\right)\left(\frac{\partial T}{\partial Y}\right)+Du\left(\xi_i^e\right)\left(\frac{\partial C}{\partial Y}\right)\right]_{Y_e}^{Y_{e+1}},$$

$$P_{ik}^{32}=Sr\int_{Y_e}^{Ye+1}\left[\left(\frac{\partial\xi_i^e}{\partial Y}\right)\left(\frac{\partial\xi_k^e}{\partial Y}\right)\right]dy, a_i^{3e}=\left[\left(\frac{\xi_i^e}{Sc}\right)\left(\frac{\partial C}{\partial Y}\right)+Sr\left(\xi_i^e\right)\left(\frac{\partial T}{\partial Y}\right)\right]_{Y_e}^{Y_{e+1}}$$

and $W_{ik}^{33}=\int_{Y_e}^{Ye+1}\left[\left(\xi_i^e\right)\left(\xi_k^e\right)\right]dy.$

In one-dimensional space, linear element, quadratic element or element of higher order can be used. The entire flow domain is divided into 10,000 quadratic elements of equal size. Each element is three-noded, and as such the whole domain contains 20,001 nodes. At each node, three functions are to be evaluated: hence, after assembling of the element equations, we got a system of 80,004 equations which are linear. Thus, an iterative scheme must be employed in the solution. On imposing the boundary conditions, a system of equations was gotten which is solved by Gauss elimination method while maintaining an accuracy of 0.00001. A convergence criterion based on the relative difference between the current and previous iterations is used. After these differences satisfy the desired accuracy, the solution is assumed to have been converged and iterative process terminated. The Gaussian quadrature is implemented for solving the integrations. The code of the algorithm has been executed twice in MAPLE for cases 1 and 2. Excellent results was seen for all results.

4. Results and Discussion

To gain insight on the effects of different parameters associated with flow field, the numerical results of the fluid velocity, temperature, concentration, Skin-friction, Nusselt and Sherwood numbers are computed numerically for both cases. Figure 1 and 2 depict the effects of thermal and mass Grashof numbers on the velocity profiles. It is observed that there is an increase in the velocity because of the enhancement of thermal buoyancy force. Also, the peak value of the velocity increases rapidly near the porous plate and the decays smoothly for free steam velocity. It is further noted that the fluid velocity increases and the peak value is more distinctive due to increase in species buoyancy force. Thus, the velocity distribution attains a

distinctive maximum value in the vicinity of the plate and then reduces properly to approach free stream value. The effect of Magnetic parameter (Hartmann number) on the velocity profiles is as presented in Figure 3. It is observed that the velocity of the fluid decreases with increasing magnetic parameter in both cases. This is due to the fact that the presence of magnetic field in an electrically conducting fluid sets in a force called Lorentz force which acts against the flow if the magnetic field is applied in the normal direction as reflected in the problem. This type of resistive force has a tendency to slow down the flow field.

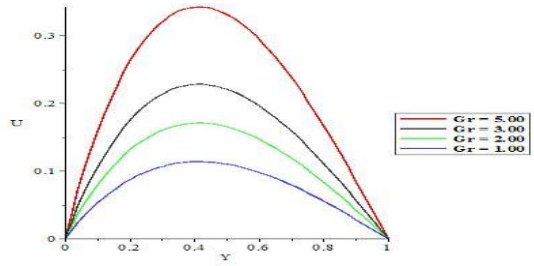

Figure 1. Velocity profiles for different values of Thermal Grashof number (Gr).

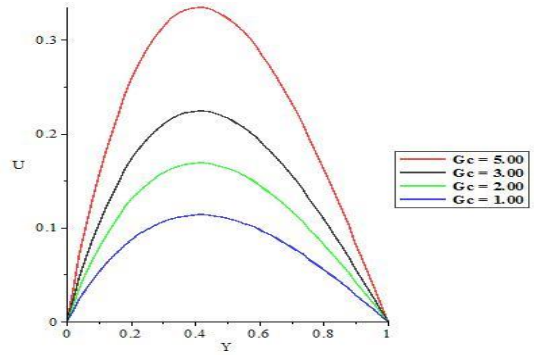

Figure 2. Velocity profiles for different values of mass Grashof number (Gc).

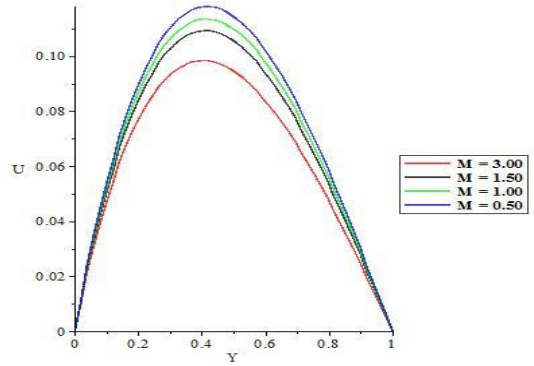

Figure 3. Velocity profiles for different values of Magnetic parameter (M).

It is revealed from Figure 4 that an increase in time leads to rise in the fluid velocity. It indicates that there is an enhancement in the fluid velocity as time progresses. Figure 5 displays the effect of Prandtl number on the velocity profiles. From this Figure, it is clear that the velocity falls as the values of Prandtl number increases. Physically, this happens because fluid with high Prandtl number have greater viscosity, which makes the fluid thick and then move slowly. The effect of Dufour number Du for different values on the velocity profiles are plotted in Figure 6. It is seen that increase in Dufour number causes a rise in the velocity throughout the boundary layer. However, a distinct velocity overshoot exists near the plate, and thereafter the profiles fall to zero at the edge of the boundary layer. Figure 7 depicts the velocity profiles for different values of Soret number. It is noticed that an increase in Soret number results in an increase in the velocity boundary layer.

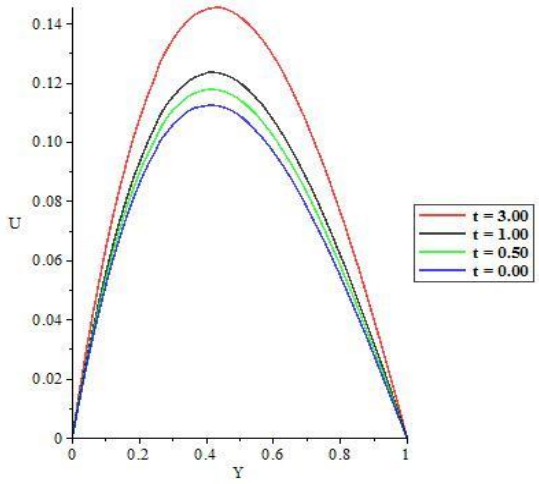

Figure 4. Velocity profiles for different values of time (t).

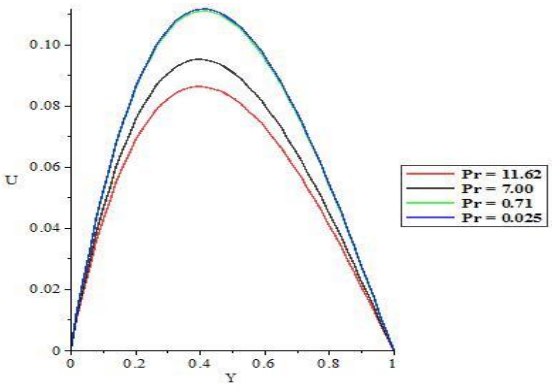

Figure 5. Velocity profiles for different values of Prandtl number (Pr).

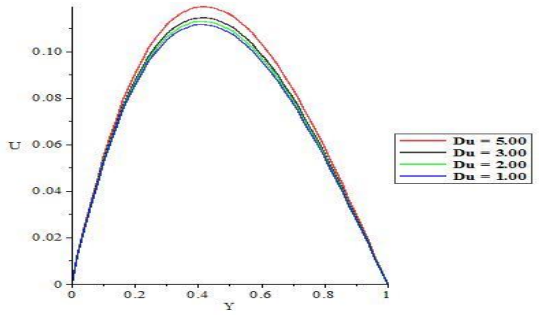

Figure 6. Velocity profiles for different values of Dufour number (Du).

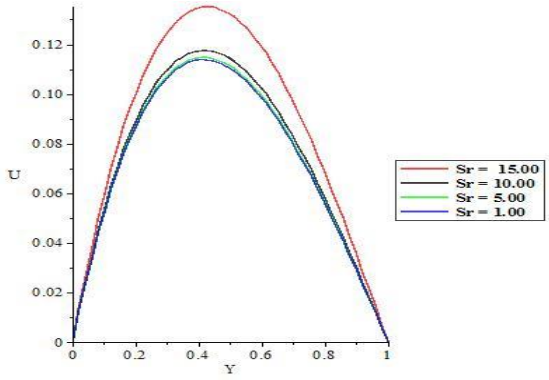

Figure 7. Velocity profiles for different values of Soret number (Sr).

Figure 8 shows the effect of Prandtl number on the temperature profiles. From this Figure, it is found that the temperature reduces as Prandtl number is increased. The effect of thermal radiation on the velocity profiles in the boundary layer is illustrated in Figure 9. It is noticed that increase in the thermal radiation parameter results in increasing velocity within the boundary layer. In Figure 10, the effect of Dufour number Du for different values on the temperature profiles are plotted. Increase in Dufour parameter causes a rise in the thermal boundary layer.

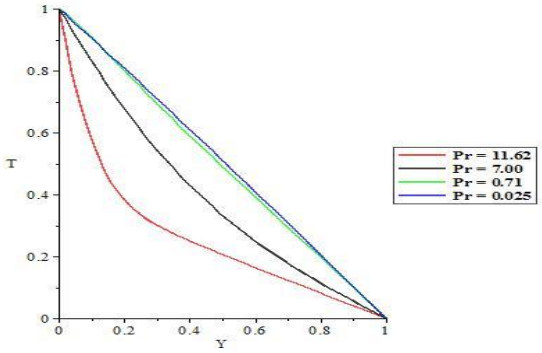

Figure 8. Temperature profiles for different values of Prandtl number (Pr).

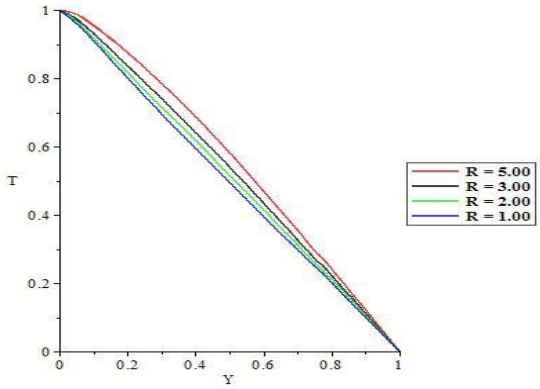

Figure 9. Temperature profiles for different values of thermal radiation parameter (R).

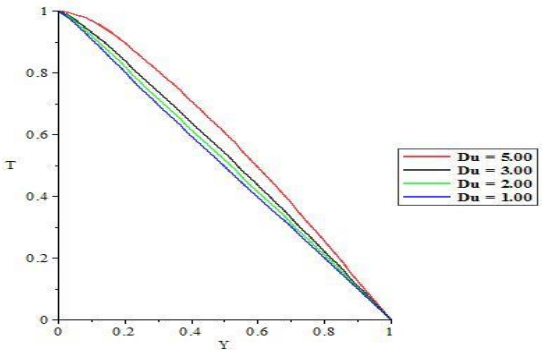

Figure 10. Temperature profiles for different values of Dufour number (Du).

Figure 11 connotes the concentration field due to variation in Schmidt number. It is observed the concentration of the fluid decreases as the Schmidt number increases. Physically, this holds due to the fact that increase in Sc means decrease of molecular diffusivity, which results in decrease of concentration boundary layer. Hence, the concentration of species is smaller for higher values of Sc.

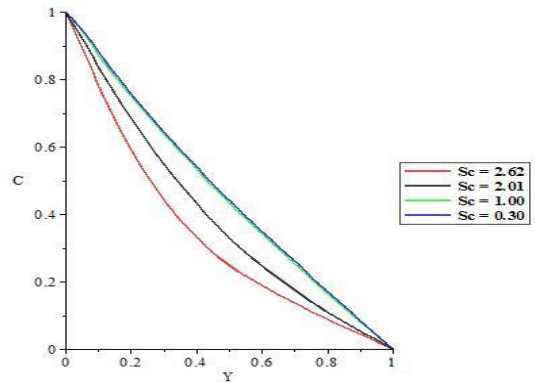

Figure 11. Temperature profiles for different values of Schmidt number (Sc).

5. Conclusion

We studied unsteady heat and mass transfer MHD convective Couette flow with thermal radiation. The problem is described by a system coupled linear partial differential equations, and it is solved by finite element method. Computations and experiments are performed to examine the effects of thermo physical parameters on the velocity, temperature and concentration profiles as well as the Skin-friction, rate of heat and mass transfer. From this study, the following conclusion are drawn:

1. The fluid concentration increases with higher Sc.
2. Increasing R and Du lead to rise in the fluid temperature while a reverse trend is found for higher $\Pr$.
3. The velocity of the fluid increases when Gr, Gc, Du and Sr are increased. The opposite is observed for higher values of $\Pr$ and M.
4. When the numerical results of the present study are compared with the previous results of [11] at $S = 0$ and $Rc = 0$ an excellent agreement was observed.

Nomenclature

H Distance between two parallel plates
B_0 Magnetic field component along y^* − axis
C_p Specific heat at constant pressure
C_s Concentration susceptibility
Gr Grashof number for heat transfer
Gc Grashof number for mass transfer
g Acceleration due to gravity
M Hartmann number
$\Pr$ Prandtl number
Sc Schmidt number
F Accelerating parameter
D Chemical molecular diffusivity
T^* Temperature of the fluid
T_w^* Temperature of the fluid near to moving plate
T_H^* Temperature of the fluid near to the stationary plate
C^* Concentration of the fluid
C_w^* Concentration of the fluid near to moving plate
C_H^* Concentration of the fluid near to the stationary plate
t^* Time in x^*, y^* coordinate system
t Time in dimensionless co-ordinate(s)
u^* Velocity component in x^* − direction
U Dimensionless velocity component in x^* − direction
NU_0 Nusselt number at the moving hot plate
NU_1 Nusselt number at the stationary plate
Sh Sherwood number
Sr Thermal diffusion
Dr Diffusion thermo
qr Radiative heat flux
x^*, y^* Coordinate system
x, Y Dimensionless coordinates
U_0 Reference velocity, Dm Mass diffusivity
T_m Mean fluid temperature, k_T Thermal diffusion ratio
k_0 Mean absorption coefficient
S Heat generation coefficient
Rc Chemical reaction coefficient

Superscript

$*$ Dimensionless properties

Subscripts

w Wall conditions, H Free stream condition

Greek Symbols

β_T Coefficient of volume expansion for heat transfer
β_m Coefficient of volume expansion for mass transfer
σ Electrical conductivity of the fluid
θ Non-dimensional temperature
ν Kinematic viscosity
ϕ Concentration of the fluid, ρ Density of the fluid
μ Viscosity, σ^* Stefan-Boltzmann constant
k^* Mean absorption coefficient

Acknowledgement

The authors are thankful to the reviewers for their valuable comments and suggestions which have further enriched this manuscript.

Conflict of Interest

The authors declare no conflict of interest.

References

[1] B. K. Jha, A. K. Samaila and A. O. Ajibade, "Natural convection Couette flow of a reactive viscous fluid in a vertical channel,"

Computational Mathematics and Modeling, vol. 24, no. 3, p. 432 – 440, 2013.

[2] H. Usman, M. S. Magami, M. Ibrahim and E. Omokhuale, "Combined Effects of Magnetic Field and Chemical Reaction on Unsteady Natural Convective Flow in a Vertical Channel," *Asian Journal of Mathematics and Computer Research,* vol. 19, no. 2, p. 87 – 100, 2017.

[3] V. M. Soundalgekar, "Free convection effects on steady MHD flow past a vertical porous plate," *Journal of Fluid Mechanics,* vol. 6, no. 3, p. 541 – 551, 1974.

[4] S. Sengupta, "Thermal diffusion effect on free convection mass transfer flow past a uniformly accelerated porous plate with heat sink," *International Journal of Mathematical Archive,* vol. 2, p. 1266 – 1273, 2011.

[5] V. Rajesh, "MHD effects on free convection and mass transfer flow through a porous medium with variable temperature," *International Journal of Applied Mechanics and Materials,* vol. 6, p. 1 – 16, 2010.

[6] M. Narahari, "An exact solution of unsteady MHD free convection flow of a radiating gas past an infinite inclined isothermal plate," *Applied Mechanics and Materials,* p. 2228 – 2233, 2012.

[7] M. Turkyilmazoglu and I. Pop, "Soret and heat source effects on unsteady Radiative MHD free convection flow from an impulsively started infinite vertical plate," *International Journal of Heat and Mass Transfer,* vol. 55, p. 7635 – 7644, 2012.

[8] M. Umamaheswar, M. C. Raju, S. V. K. Varma and J. GireeshKumar, "Numerical Investigation of MHD free convection flow of a non-Newtonian fluid past an impulsively started vertical plate in the presence of thermal diffusion and radiation absorption," *Alexandra Engineering Journal,* vol. 55, p. 2005 – 2014, 2014.

[9] M. Archaya, G. C. Desh and P. L. Singh, "Magnetic field effects on free convection and mass transfer flow through porous medium with constant suction and heat flux," *Indian Journal of Pure and Applied Mathematics,* vol. 31, no. 1, p. 1 – 18, 2000.

[10] J. A. Chamkha, "Unsteady MHD convective heat and mass transfer flow past a semi-infinite vertical permeable moving plate with heat absorption," *International Journal of Engineering Science,* vol. 38, p. 217 – 230, 2004.

[11] R. S. Raju, G. J. Reddy, J. A. Rao and M. M. Rashidi, "Thermal diffusion and diffusion thermo effects on an unsteady heat and mass transfer Magnetohydrodynamic natural convection Couette flow using FEM," *Journal of Computational Design and Engineering,* vol. 3, p. 349 – 362, 2016.

[12] D. Chaughan and P. Rastogi, "Heat transfer effects on a rotating MHD Cuoette flow in a channel partially by a porous medium with hall current," *Journal of Applied Science and Engineering,* vol. 15, no. 3, p. 281 – 290, 2012.

[13] F. A. Salama, "Convective heat and mass transfer in a non-newtonian flow formation in a Couette motion in magnetohydrodynamic with time-varying suction," *Journal of Thermal Science,* vol. 15, no. 3, p. 749 – 758, 2011.

[14] C. Khan, K. Rakesh and S. Shavnam, "Hydro-magnetic oscillatory vertical Couette flow of radiating fluid through porous medium with slip and jump boundary conditions," *International Journal of Physical and Mathematical Sciences,* vol. 3, no. 1, p. 82 – 90, 2012.

[15] B. K. Jha, B. Y. Isah and I. J. Uwanta, "Unsteady MHD free convective Couette flow between vertical porous plates with thermal radiation," *Journal of King Saud University – Science,* vol. 27, p. 338 – 348, 2015.

[16] I. J. Uwanta and E. Omokhuale, "Viscoelastic Fluid Flow in a Fixed Plane with Heat and Mass Transfer," *Research Journal of Mathematics and Statistics,* vol. 4, no. 3, pp. 63-69, 2012.

[17] K. K. Asogwa, J. I. Uwanta, A. A. Momoh and E. Omokhuale, "Heat and Mass Transfer over a Vertical Plate with Periodic Suction and Heat Sink," *Research Journal of Applied Sciences, Engineering and Technology,* vol. 5, no. 1, pp. 07-15, 2013.

[18] I. J. Uwanta and E. Omokhuale, "Effects of Variable Thermal Conductivity on Heat and Mass Transfer with Jeffery Fluid,"

International Journal of Mathematical Achive, vol. 5, no. 3, p. 135 – 149, 2014.

[19] I. J. Uwanta, S. K. Ahmad and E. Omokhuale, "Effect of Jeffery Fluid on Heat and Mass Transfer past a Vertical Porous Plate with Soret and Variable Thermal Conductivity," *Journal of Mathematics and Computational Science,* vol. 4, no. 5, p. 915 – 939, 2014.

[20] E. Omokhuale, M. M. Altine and S. M. Ishaya, "Effects of Dufour and Heat Source on Free Convection Flow of Kuvshinshiki Fluid in a Porous Medium," *The Journal of the Mathematical Association of Nigeria (Abacus), Mathematics Science Series,* vol. 44, no. 2, p. 199 – 207, 2017.

[21] J. A. Rao, R. S. Raju and S. Sivaiah, "Finite element solution of heat and mass transfer in MHD flow of a viscous fluid past a vertical plate under oscillating suction velocity," *Journal of Applied Fluid Mechanics,* vol. 5, no. 3, p. 1 – 10, 2012.

[22] G. J. Reddy, "Unsteady MHD heat transfer in Couette flow of water at 4oC in a rotating system with ramped temperature using finite element method," *International Journal of Applied Mechanics and Engineering,* vol. 22, no. 1, p. 145 – 161, 2017.

[23] V. M. Job and S. R. Gunakala, "Finite element analysis of unsteady radiative MHD natural convection Couette flow between permeable plates with viscous and joule dissipation," *International Journal of Pure and Applied Mathematics,* vol. 99, no. 2, p. 123 – 143, 2015.

[24] B. Y. Isah, B. K. Jha and J. Lin, "On a Couette flow of conducting fluid," *International Journal of Theoretical and Applied Mathematics,* vol. 4, no. 1, p. 8 – 21, 2018.

